

# Cation substitution and strain screening in framework structures: The role of rigid unit modes

Andrew L. Goodwin<sup>a</sup>, Stephen A. Wells<sup>a,b</sup>, Martin T. Dove<sup>a,\*</sup>

<sup>a</sup> Department of Earth Sciences, Cambridge University, Downing Street, Cambridge CB2 3EQ, U.K.

<sup>b</sup> Bateman Physical Sciences PSF 359, Arizona State University, Tempe, AZ 85287-1504, U.S.A.

Accepted 16 August 2005

## Abstract

We use a combination of real-space geometric algebra and reciprocal space dynamical matrix analyses to study the effect of cation substitution on the framework geometries of  $\beta$ -quartz, cordierite and leucite. We show that the geometric stress associated with the substitution in these framework silicates is absorbed by rigid-unit type motion of those coordination polyhedra near the substitution site. We find that the inherent flexibility of these structures enables screening of geometric stress, such that the associated energy cost is minimal and unlikely to influence substitution patterns.

© 2005 Elsevier B.V. All rights reserved.

PACS: 61.72.-y; 63.20.Pw

Keywords: Al–Si ordering; Silicates; Geometric algebra; Rigid unit modes; Strain screening; Framework structures

## 1. Introduction

Cation substitution is a phenomenon observed repeatedly throughout both naturally occurring and synthetic framework materials; in particular, Al-substituted (‘stuffed’) silicates and zeolites are a class of materials of great importance to the earth sciences. The substitution patterns exhibited by these materials are varied, and can involve order (or disorder) on multiple length scales. However, some empirical rules do emerge. For example, the ‘Al-avoidance rule’ reflects the observation that Al atoms rarely substitute the centres of connected  $[\text{SiO}_4]$  tetrahedra in framework silicates. In general, such rules are qualitatively explained in terms of two balanced effects. The first considers the electrostatic interaction

between substituted centres; for example, the  $[\text{AlO}_4]$  coordination polyhedra in siliceous frameworks bear a negative charge, and so the substitution of adjacent coordination polyhedra carries with it a large electrostatic energy cost. The second is a geometric effect, which accounts for the strain introduced by the associated change in metal–oxygen bond lengths.

Taken at face value, the suggestion that one can minimise the geometric strain associated with Al-substitution by maximising the number of Al–O–Si linkages seems a natural assumption. However, the manner in which such geometric strains propagate throughout the crystal lattice, and their effect on possible substitution patterns are non-trivial issues. To address these, it is important to explore the way in which framework structures respond to the introduction of substitutional centres. Such a response will necessarily depend on the inherent flexibility of the framework; i.e., the degree to which the framework can distort with minimal energy cost.

\* Corresponding author. Tel.: +44 1223 333 482; fax: +44 1223 333 450.

E-mail address: martin@esc.cam.ac.uk (M.T. Dove).

A simple and surprisingly effective interpretation of framework flexibility is that given by the Rigid Unit Mode (RUM) model. In this picture, the metal coordination polyhedra within the framework are viewed as rigid units, connected to form the required framework topology. The physical significance of the model lies in the observation that the forces required to deform coordination geometries are significantly greater than those required to rotate and/or translate coordination polyhedra relative to each other. The various combinations of translations and rotations of the rigid units that preserve the framework topology, such as the octahedral rotation mode in perovskite (Fig. 1), are consequently likely to dominate the dynamical behaviour of the material. Indeed, those phonon modes that can be described in this way (termed RUMs) often occur at very low energy (typically 0–2 THz) and so dictate many physical properties of the materials in which they exist. The model has enjoyed much success in explaining a range of phenomena, including the existence and nature of phase transitions (Hammonds et al., 1996) and anomalous thermal expansion behaviour (Heine et al., 1999; Welche et al., 1998).

In this paper, we show that the topologies of a number of framework structures are capable of accommodating cation substitution without significant deformation of individual coordination polyhedra. In particular, the associated geometric ‘stress’ can be absorbed by the rotations and/or translations of the neighbouring coordination polyhedra. The same inherent framework flexibility that gives rise to RUM-type vibrational motion is shown to allow cation substitution with a small geometric energy cost.

Our analysis involves the use of two methods: firstly, a recently developed geometric algebra approach that quantifies the influence of rigid-unit motion on atomistic configurations; secondly, a novel dynamical

matrix method that determines the flexibility of each framework with respect to changes in size (‘breathing’) of the coordination polyhedra. We present results for three representative silicate structures:  $\beta$ -quartz, cordierite and leucite.

## 2. Geometric algebra analysis

Despite the obvious usefulness of the RUM model in determining the dominant reciprocal-space influences on framework structures, the active phonon modes in a real material do not in practice fall neatly into a family of RUMs that dominate all motion, and another family of non-RUMs with minimal effect on atomic displacements. Instead, any mode can include components of either type of motion, with the relative proportions varying primarily as a function of mode frequency. As such, atomistic configurations – ‘snapshots’ of instantaneous atomic positions within a material – will reflect the influence of both RUM- and non-RUM-type phonon modes.

To quantify these contributions, a real-space analysis of RUM fluctuations based on the technique of geometric algebra (GA) has recently been developed (Wells et al., 2002) and has been implemented by the program GASP (Wells et al., 2004; Wells, 2004). It allows us to determine the extent to which atomistic configurations can be described in terms of RUM displacements, by decomposing the atomic displacements into rigid-unit translations, rotations and distortions.

The approach compares the polyhedral geometries within a given structure, before and after introduction of the defect. Let  $A$  denote any one polyhedron in the initial configuration and  $A'$  the corresponding polyhedron in the defective structure. If  $A$  and  $A'$  are superposed such that their centres coincide, there will be a mismatch between each vertex  $Q$  of  $A$  and the

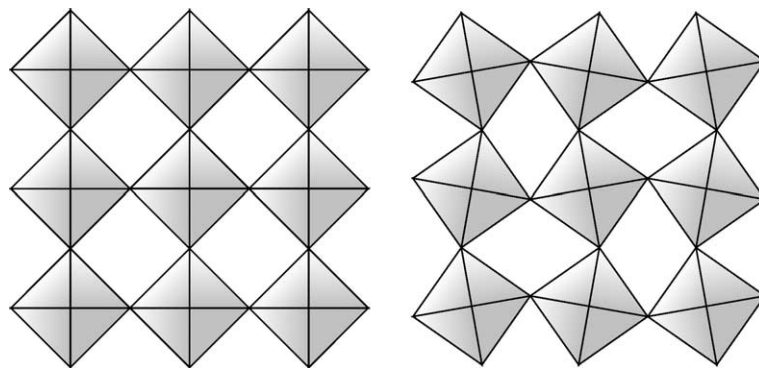


Fig. 1. Illustration of a rigid unit mode in the perovskite structure. The mode involves counter-rotation of successive coordination octahedra about an axis perpendicular to the page, and preserves the integrity of all coordination polyhedral geometries.

corresponding vertex  $Q'$  of  $A'$  given by the vector  $d\mathbf{r} = \mathbf{r}(Q) - \mathbf{r}(Q')$ . The sum of the squares of the mismatches over all vertices ( $\sum_Q |d\mathbf{r}|^2$ ) is a measure of the difference between  $A$  and  $A'$ . If we now allow  $A$  to rotate freely, we can minimise this sum-of-squares mismatch score until the orientation of  $A$  matches that of  $A'$ . The residual mismatch score after this operation measures the distortion of  $A'$  relative to  $A$ .

The residual mismatch for each vertex can be resolved into components parallel and perpendicular to the (reoriented) bond vector, corresponding to stretching of the Si–O bond and bending of the intra-polyhedral O–Si–O angles, respectively. Consequently, for each polyhedron, we can quote both RMS bending and RMS stretching distortions, which together quantify the total alteration to the polyhedral geometry. A convenient property of the geometric analysis is that both stretching and bending distortions are measured in Ångströms and so can be compared directly.

The rotation of the polyhedron  $A$  to most closely match the orientation of  $A'$  is given by a rotor object  $\mathbf{B}$  with three Cartesian components  $B_x, B_y, B_z$ , such that the axis of the rotation is parallel to the vector  $[B_x, B_y, B_z]$  and has magnitude  $\theta = 2 \arcsin\left(\frac{|\mathbf{B}|}{2}\right)$ . To first order, the three components measure the rotation of the polyhedron about the Cartesian axes.

### 2.1. Mott–Littleton configurations

One method of generating appropriate atomistic configurations of substituted silica frameworks is that of Mott and Littleton—as coded into the general modelling program GULP (Gale, 1997). This approach uses empirical interatomic potentials, and relaxes the structure around a defect site up to a pre-defined cut-off. The remaining region is approximated as a polarizable medium.

An Al centre was introduced into configurations of both SiO<sub>2</sub>-cordierite and  $\beta$ -quartz. Each configuration was relaxed to a cut-off radius of 15 Å, and the output analysed using GASP. The results, illustrated in Fig. 2, indicate two effects: firstly, a significant degree of atomic motion is required to accommodate the defect—particularly in the case of  $\beta$ -quartz—and, secondly, that the bulk of this motion is attributable to rigid-unit rotations and translations.

### 2.2. Rigid-ion configurations

The large cut-off radius required and the fact that a number of rigid units necessarily span both the relaxed (inner) and polarizable (outer) regions are both computational problems for the Mott–Littleton approach. Con-

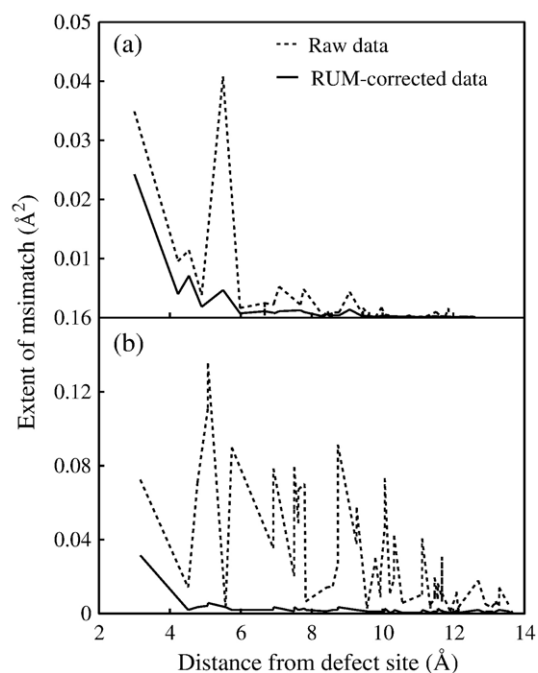


Fig. 2. Distortion in the (a) SiO<sub>2</sub>-cordierite and (b)  $\beta$ -quartz frameworks induced by an Al-substitution event. The dashed lines represent total distortion values based on atomic displacements; the solid lines give the residual deformation after taking account of the RUM component of the atomic displacements, as determined by GA analysis of our Mott–Littleton atomistic simulation. Such motion clearly accounts for a large fraction of the structural response of the framework to the substitutional defect. (Top panel adapted from (Wells et al., 2002))

sequently, we chose to balance our analysis by considering configurations generated using a standard rigid-ion model. In this instance, it was necessary to counter the negative charge of the Al-substituted frameworks with a monovalent cation (Li<sup>+</sup>). We used the potential of Calleja et al. (2001) to relax a configuration representing a  $6 \times 6 \times 6$  supercell of  $\beta$ -quartz. Conveniently this particular potential, which is based on the silica model of Kramer et al. (1991) with an added Li–O term from LiAlSi<sub>2</sub>O<sub>6</sub>, had been designed specifically for use with Li/Al-substituted quartz configurations.

The incorporation of a Li<sup>+</sup> ion within the general structure imparts an electrostatic effect to the overall framework response. This effect is particularly noticeable in the geometry of the [SiO<sub>4</sub>] coordination tetrahedron immediately adjacent to the Li<sup>+</sup> site. Indeed, the Li/Al defect effectively takes the form of an Al–[O<sub>2</sub>]–Li–[O<sub>2</sub>]–Si moiety, in which the Si–O coordination geometries are highly distorted. In analysing these configurations, it is possible then to observe how the silicate framework responds to both the incorporation of the Al centre and the Li<sup>+</sup>-induced distortion of the proximal [SiO<sub>4</sub>] unit.

Our results (illustrated in Fig. 3) show that the rigid unit distortions are localised to the few neighbouring polyhedra of both the substitution site and the proximal  $[\text{SiO}_4]$  unit. Again, it was possible to interpret the remainder of the framework response largely in terms of rotations and translations of rigid units. The extent of both rigid-unit motion and distortion decayed rapidly with increasing displacement from the  $\text{Li}^+$  site. Indeed, this behaviour mirrors that observed in the configurations generated using the Mott–Littleton approach.

### 2.3. Cation exchange energies

In a series of papers, summarised by Bosenick et al. (2001), our group has studied the energetics of Al/Si cation ordering in framework silicates. It is generally found that the energy of a configuration can be expressed in the form

$$E = \sum_{\langle i,j \rangle} J_{ij} S_i S_j \quad (1)$$

where  $S_i$  is a variable with value 1 if the site  $i$  contains an Al cation, or 0 otherwise. The coefficients  $J_{ij}$  are the

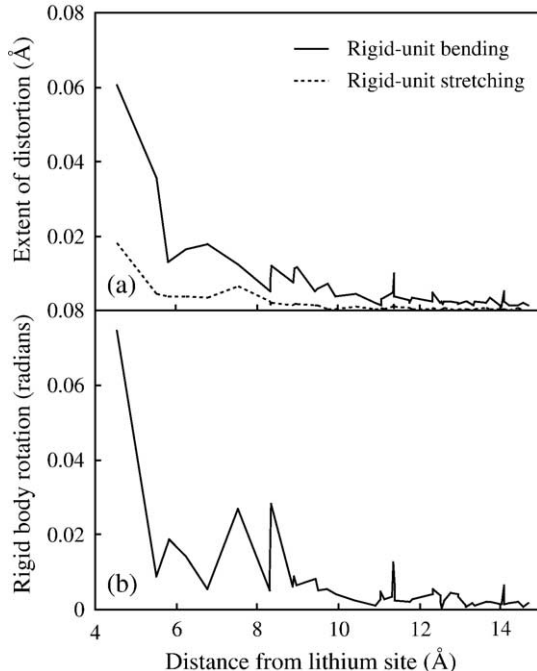


Fig. 3. Rigid-unit response to Li/Al substitution in the  $\beta$ -quartz framework as determined by GA analysis of our rigid-ion atomistic simulation. The extent of rigid-unit distortion (a) [separated into bending (solid line) and stretching (broken line) components] and rotation (b) decays rapidly for successively distant rigid unit neighbours of the  $\text{Li}^+$  site.

exchange energies. Bosenick et al. (2001) compare values of  $J$  for nearest neighbour distances for a range of aluminosilicates, and find more variability than would be expected if the interaction were to arise purely from electrostatic effects. This variability is attributed to the role of strain.

Values of  $J$  for more distant neighbours appear to have no trends, and indeed can have positive or negative values. Typical values are much smaller than the value of  $J$  for nearest-neighbour interactions. Bosenick et al. (2001) compare values for second and third neighbour interactions around 6-membered rings of tetrahedra in several different systems. We make two observations from Fig. 2. First, strain screening clearly operates over the length scale of second-neighbour distances and beyond, which explains why values of  $J$  for these interactions are much lower than for the nearest-neighbour interaction. However, the analysis in this section ignores effects such as the energy associated with flexing of the Si–O–Si bond, and we propose that it is these interactions, rather than strain propagating through the tetrahedra, that determines the magnitude of the higher-neighbour exchange energies.

### 3. Breathing RUM analysis

Real-space analyses of framework flexibility, such as those presented above, are useful in visualising the ability of frameworks to accommodate substitutional centres. However, they necessarily involve the use of a handful of individual configurations and so lose in generality what they gain in clarity. We describe here a complementary approach in which the general nature of framework flexibility is elucidated in terms of a reciprocal-space view of framework structures.

#### 3.1. Split-atom approach

For a given framework structure, the number and nature of the RUMs that it is capable of supporting depend in a non-trivial manner on its topology. Indeed, their determination is generally too difficult a task to be performed by inspection alone. Rather, the method of choice is a dynamical matrix approach, automated by the freely available program CRUSH (Giddy et al., 1993; Hammonds et al., 1994).

The approach used by this program reduces a given framework structure to its constituent coordination polyhedra (the rigid units). Each unit  $j$  is assigned six degrees of freedom: three translational (assembled into a translation vector  $\mathbf{u}_j$ ) and three rotational (which characterise the  $3 \times 3$  rotation matrix  $\mathbf{R}_j$ ). The points

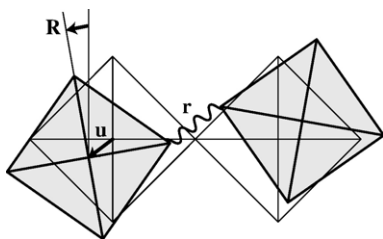


Fig. 4. Representation of the split-atom model used to construct the dynamical matrix. Each rigid unit possesses six degrees of freedom: three translational (the elements of the translation vector  $\mathbf{u}$ ) and three rotational (the elements of the rotation matrix  $\mathbf{R}$ ). The energy term  $\varphi$  of the model depends on the separation  $\mathbf{r}$  between split atoms and is zero if and only if the polyhedral connectivity is preserved.

at which the rigid units are connected correspond to bridging oxygen atoms in the original (atomistic) structure. These atoms are then split between the two units they bridge, and the resulting pair is connected by a fictitious spring of zero equilibrium length (Fig. 4).

The energy term  $\varphi$  associated with this spring then depends on the separation  $\mathbf{r}$  of the two split atoms:

$$\varphi(\mathbf{r}) = \frac{1}{2}K|\mathbf{r}|^2 \quad (2)$$

where

$$\mathbf{r} = \mathbf{u}_1 - \mathbf{u}_2 + \mathbf{R}_1 \cdot \mathbf{e}_1 - \mathbf{e}_1 - \mathbf{R}_2 \cdot \mathbf{e}_2 + \mathbf{e}_2 \quad (3)$$

Here, the  $\mathbf{e}_i$  are the vectors joining the split atoms to the centre of their respective rigid units.

In this way, the geometry of the rigid units is preserved as a strict constraint, whilst the connectivity of the framework is treated as a slack constraint. The force constant  $K$  is the only variable in the model and would have infinite value if we were to impose a strict connectivity constraint. It represents—to a first-order approximation—the force required to deform the rigid units, and can be tuned to correlate with appropriate

experimental values. The interaction energies  $\varphi$  defined in this way can be assembled in the usual manner into a dynamical matrix, whose eigenvalues are related to the mode frequencies (Dove, 1993). A mode will be calculated to have zero frequency if and only if it does not involve any separation in the split atoms; i.e., it is a RUM. Moreover, the eigenvectors of these modes will describe the motion of the various rigid units associated with the mode.

### 3.2. The breathing RUM model

In order to extend this model to one with which we might study the effects of cation substitution, we assign to each rigid unit one additional degree of freedom: a breathing factor  $\rho$ , which corresponds to a scaling of the rigid unit size. In physical terms, the scaling of a  $[\text{SiO}_4]$  tetrahedron by an appropriate factor could represent its replacement by the larger  $[\text{AlO}_4]$  species. The appropriate formalism corresponding to Eq. (3) is then given by:

$$\mathbf{r} = \mathbf{u}_1 - \mathbf{u}_2 + (1 + \rho_1)\mathbf{R}_1 \cdot \mathbf{e}_1 - \mathbf{e}_1(1 + \rho_2)\mathbf{R}_2 \cdot \mathbf{e}_2 + \mathbf{e}_2 \quad (4)$$

The construction and analysis of the corresponding dynamical matrix differs from the standard split-atom approach predominantly in the order of the constituent blocks (having increased from 6 to 7) and the interpretation of the eigenvectors (one component of which will correspond to the breathing factor  $\rho$ ). The set of modes with zero-valued frequencies will contain the family of RUMs obtainable through the standard split-atom approach, together with a collection of breathing RUMs (BRUMs)—modes that involve changes in the polyhedral sizes (an example of which is given in Fig. 5).

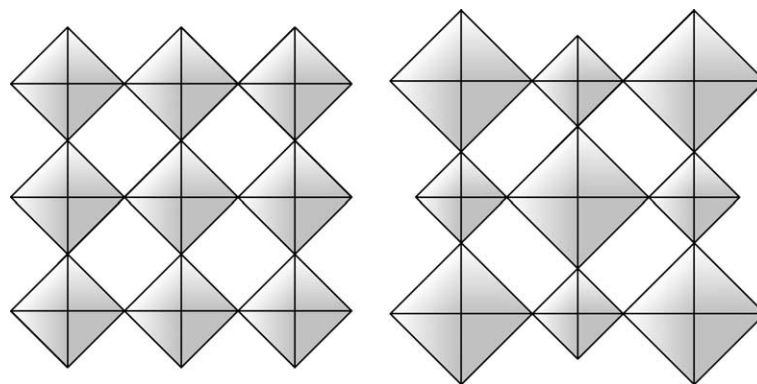


Fig. 5. Illustration of a BRUM in the perovskite structure. The coordination octahedra are alternately magnified and reduced by the same factor. As for the RUM shown in Fig. 1, the mode preserves the integrity of all coordination polyhedral geometries.

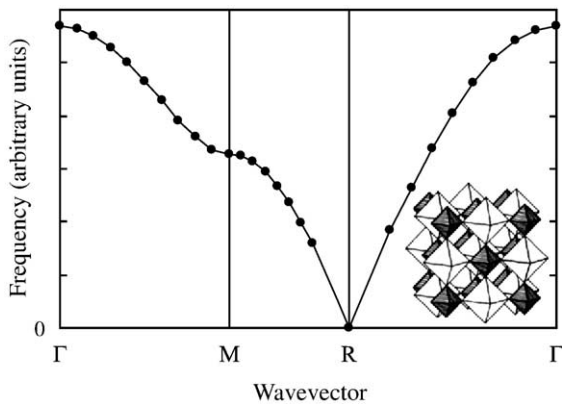


Fig. 6. Wave vector dependence of the nominal breathing mode frequency in the perovskite structure. The mode frequency falls to zero at the *R* point, where it corresponds to a BRUM. The physical interpretation of this BRUM is a substitution pattern in which the coordination octahedra alternate in size throughout the structure (inset).

As an illustration of the physical meaning of this extension to the model, we consider initially the perovskite structure. In this instance, the unit cell contains a single rigid unit, and so the dynamics are described in terms of seven phonon modes, at least one of which will involve the breathing motion described above. The wave vector dependence of the frequency of this mode along the high symmetry directions is shown in Fig. 6. As the mode itself is hypothetical, the absolute energy values determined by the program are arbitrary and have no physical significance. What is important, however, is the relative behaviour of the dispersion curve. In particular, the breathing mode frequency falls to zero at the *R* point, illustrating the presence of a BRUM at this wave vector (in addition to the triply-degenerate rotational RUM at the same wave vector). Inspection of the associated eigenvector indicates that the mode represents alternate magnification and reduction of the coordination octahedra throughout the structure; this is essentially the three-dimensional analogue of the substitution pattern illustrated in Fig. 5 (inset to Fig. 6).

The perovskite structure is a particularly simple system; for more complex structures, one often observes significant mixing between the standard RUMs and any BRUMs that might occur such that all zero-frequency modes appear to possess some breathing component. Consequently, it can prove difficult to interpret the mode eigenvectors in a physically sensible manner. Importantly, the total number of zero-frequency modes  $n_{\text{BRUM}+\text{RUM}}$  can be easily determined and is unaltered by any mixing between the two types of zero-frequency modes. By using both the original split-atom and breathing approaches separately, we can confident-

ly arrive at the additional number of breathing rums  $n_{\text{BRUM}}$  at any given wave vector:

$$n_{\text{BRUM}} = n_{\text{BRUM}+\text{RUM}} - n_{\text{RUM}} \quad (5)$$

where  $n_{\text{RUM}}$  is the number of RUMs determined using the original split-atom approach. As we explore further below, the ratio of the quantity  $n_{\text{BRUM}}$  to the number of rigid units themselves can be related directly to the flexibility of the framework with respect to cation substitution.

### 3.3. Practical implementation

A modified version of the original crush program, referred to here as B-CRUSH, is used to calculate the breathing mode frequencies and eigenvectors (in addition, of course, to those of the standard translational and rotational modes) according to the theoretical framework given above. The use of a single breathing parameter carries with it an inherent isotropy that can result in slight yet persistent errors when polyhedra with non-ideal geometries are used. Consequently, these geometries for a given structure are initially modified using the program IDEALISER (Hammonds and Dove, 1998) prior to analysis by B-CRUSH. IDEALISER attempts to regularise all coordination polyhedra in the given structure; i.e., to give tetrahedral O–Si–O angles of  $109.5^\circ$  and equal Si–O bond lengths. To do so, one allows the program a certain degree of flexibility in parameters such as the unit cell lengths and Si–O–Si angles. The framework topology remains unaltered throughout this process, and so the B-CRUSH output is equally applicable to the original non-ideal structure as it is to the newly generated idealised structure.

### 3.4. Analysis of framework silicates

The number of BRUMs across the entire Brillouin zone (BZ) was determined at a resolution of  $k/20$  in the relative wave vector for  $\beta$ -quartz, cordierite and leucite. The results are summarised in Table 1. In contrast to the perovskite structure, which we have already seen to be incapable of supporting BRUMs at wave vectors other

Table 1  
Number of breathing RUMs at any wave vector for some framework materials

Material	Number of rigid units per unit cell	$n_{\text{BRUM}}$
$\beta$ -quartz	3	3
Cordierite	36	36
Leucite	48	48
Perovskite	1	0

than the  $R$  point, the value of  $n_{\text{BRUM}}$  for each framework silicate was found to equal the number of rigid units in the unit cell at all values of the wave vector. This somewhat unexpected result has immediate implications regarding the ability of these frameworks to accommodate substitutional centres.

The breathing motion for each rigid unit in our model is described completely by one degree of freedom; consequently, we find that the number of BRUMs in the silicate frameworks is precisely equal to the number of breathing degrees of freedom. It follows that the breathing motion of any one polyhedron in the structure can be decoupled from that of all other polyhedra. It is convenient to consider this occurring with an appropriate wave packet—a superposition of the BRUMs at appropriate wave vectors. Upon variation of the size of any given polyhedron (corresponding to a single substitution ‘event’), the entire set of rigid units within the framework can be rotated and/or translated such that (i) the geometric integrity of all rigid units is retained and (ii) the connectivity of the framework structure is preserved.

Disappointingly, our analysis does not easily yield the explicit nature of these rigid-unit rotations and translations. To see why this is the case, we consider the breathing ‘motion’ associated with a given wave packet. The breathing ‘motion’  $\rho_j(\mathbf{r})$  of the rigid unit  $j$  at position  $\mathbf{r}$  can be expressed as a sum of contributions from the BRUMs  $\nu$  of the wave packet across the BZ:

$$\rho_j(\mathbf{r}) = \sum_{k \in \text{BZ}, \nu} \lambda(\mathbf{k}, \nu) \rho_j(\mathbf{k}, \nu) \exp[i\mathbf{k} \cdot \mathbf{r}] \quad (6)$$

Here, the  $\rho_j(\mathbf{k}, \nu)$  are the breathing components of the relevant mode eigenvectors (calculated by B-CRUSH), and the  $\lambda(\mathbf{k}, \nu)$  their weightings. The mode eigenvectors are independent of the chosen wave packet, but the mode weightings are not: it is their values that we must calculate to characterise the rigid-unit motions involved. Once their value is known, the  $\lambda(\mathbf{k}, \nu)$  yield the translation vectors and rotation matrices for each rigid unit:

$$\mathbf{u}_j(\mathbf{r}) = \sum_{k \in \text{BZ}, \nu} \lambda(k, \nu) \mathbf{u}_j(k, \nu) \exp[i\mathbf{k} \cdot \mathbf{r}] \quad (7)$$

$$\mathbf{R}_j(\mathbf{r}) = \sum_{k \in \text{BZ}, \nu} \lambda(\mathbf{k}, \nu) \mathbf{R}_j(\mathbf{k}, \nu) \exp[i\mathbf{k} \cdot \mathbf{r}] \quad (8)$$

For all rigid units  $\{j, \mathbf{r}\}$ , we have  $\rho_j(\mathbf{r})=0$  except for the one particular rigid unit  $\{j', \mathbf{r}'\}$ , whose size is allowed to change: in its case,  $\rho_{j'}(\mathbf{r}')=1$ . Using this information, it is possible—in principle—to evaluate

the  $\lambda(\mathbf{k}, \nu)$ . From a simple variable-counting perspective, we have as many unknowns—the  $\lambda(\mathbf{k}, \nu)$ —as we have relations given by the general Eq. (5). This is the case only because there is a one-to-one relationship between BRUMs at arbitrary wave vector and rigid units in the unit cell. However, the calculation suffers from a need to place a limit on the number of unit cells that we consider in our model. Termination at some

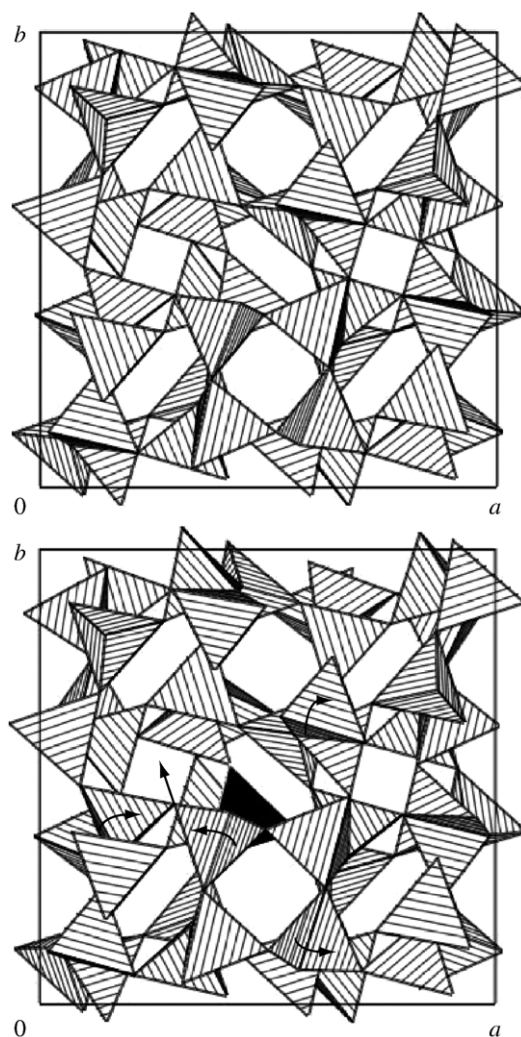


Fig. 7. Accommodation of cation substitution within the leucite structure as determined by IDEALISER. The top panel shows the positions of rigid units within the native unit cell. The geometries of the units have been regularised so that all O–Si–O angles are  $109.5^\circ$  and all Si–O bond lengths are equal. One tetrahedron (coloured black) in the structure is enlarged to reflect the substitution of a Si atom by an Al atom. The configuration is again regularised; however the Al–O and Si–O bond lengths are constrained to differ by  $0.1 \text{ \AA}$ . The configuration determined by IDEALISER (bottom panel) illustrates how the coordination polyhedra within the structure can be seen to rotate and translate to accommodate the geometric stress associated with the cation substitution.

arbitrarily large value of  $|r|$  carries with it the inherent assumption that no associated RUM-type motion occurs at distances greater than this value. This is difficult to assess *a priori*.

To some extent, the results obtained from the breathing RUM approach are non-constructive: they predict that the framework silicates studied are geometrically capable of accommodating substitutional centres without significant distortion to their constituent rigid units but do not explicitly illustrate how they manage to do so. Nonetheless, they do provide an unambiguous indication that these structures are incredibly flexible and that this flexibility does not only have the potential to influence their dynamical properties, but also their ability to incorporate cation substitution.

The motivation for the BRUM model arises from the expectation, as shown in the previous section, that strain associated with ordering within the aluminosilicate network would be accommodated through RUM deformations of the network. By incorporating a variable associated with cation size, which translates to tetrahedron size, it is possible to develop a dynamical model in which variations in cation size are coupled with RUM motions. For example, Al/Si ordering in a material such as cordierite could be correlated with rotations of the tetrahedra. It was anticipated, with overdue optimism as it now turns out, that a subset of zero frequency solutions to the new model would contain the ordering patterns observed experimentally.

#### 4. Discussion

The inherent flexibility of framework silicates is now widely appreciated and is indeed manifest in many other properties of these materials. For example, an investigation into the mechanism of ion conduction within framework silicates (Sartbaeva et al., 2004) illustrates that the cross-channel widths in the  $\beta$ -quartz structure can be varied by distances as large as 0.5 Å with a concomitant energy cost of less than 0.5 eV. Again, the movement is shown to be accommodated by collective motion of the polyhedra within the framework.

It is also possible to use the program IDEALISER to examine (in real-space) the geometric effects of cation substitution. As discussed above, the program attempts to regularise all the coordination polyhedra in a given structure. Of relevance to the present study is the ability to constrain the bond lengths within different tetrahedra in different ways. In particular, it is possible to force one tetrahedron within a framework silicate structure to be larger than all others (each of which are constrained

to have the same size). The resulting configuration—if one can be found by the program—corresponds directly to the wave packet considered in our reciprocal space analysis above.

For example, IDEALISER successfully finds a solution when given the atomic coordinates of leucite and the Si–O bond lengths within a single  $[\text{SiO}_4]$  tetrahedron are constrained to be 0.1 Å longer than those in the rest of the structure (as indeed it does for supercells of  $\beta$ -quartz and cordierite). The resulting configuration is illustrated in Fig. 7 and reveals the method by which the ensemble of coordination tetrahedra are capable of absorbing the substitutional centre through rigid-unit translations and rotations.

In summary, we have shown that a number of framework silicates are capable of accommodating substitutional centres with minimal distortion to the coordination polyhedra that constitute the framework geometry. The energy associated with action substitution is generally determined by a mixture of electrostatic interactions and the energies associated with flexing of (Al/Si)–O–(Al/Si) bonds or equivalent, rather than by deformation of the structural polyhedra. The only case where polyhedral distortion will play a role is in the nearest-neighbour interaction. Strain screening lowers the energy cost of substitutions or disordering processes, and dampens the length scales over which strain associated with cation substitution will propagate.

#### Acknowledgments

A.L.G. acknowledges financial support from Trinity College, Cambridge, U.K. [LW]

#### References

- Bosenick, A., Dove, M.T., Myers, E.R., Palin, E.J., Sainz-Diaz, C.I., Guiton, B.S., Warren, M.C., Craig, M.S., Redfern, S.A.T., 2001. Computational methods for the study of energies of cation distributions: applications to cation-ordering phase transitions and solid solutions. *Mineral. Mag.* 65 (2), 193–219.
- Calleja, M., Dove, M.T., Salje, E.K.H., 2001. Anisotropic ionic transport in quartz: the effect of twin boundaries. *J. Phys. Condens. Matter* 13 (42), 9445–9454.
- Dove, M.T., 1993. *Introduction to Lattice Dynamics*. Cambridge University Press, Cambridge.
- Gale, J.D., 1997. GULP: A computer program for the symmetry-adapted simulation of solids. *J. Chem. Soc., Faraday Trans* 93 (4), 629–637.
- Giddy, A.P., Dove, M.T., Pawley, G.S., Heine, V., 1993. The determination of rigid-unit modes as potential soft modes for displacive phase transitions in framework crystal structures. *Acta Crystallogr., Sect. A* 49 (5), 697–703.
- Hammonds, K.D., Dove, M.T., 1998. IDEALISER. [http://www.esc.cam.ac.uk/mineral\\_sciences/crush/](http://www.esc.cam.ac.uk/mineral_sciences/crush/).



- Hammonds, K.D., Dove, M.T., Giddy, A.P., Heine, V., 1994. Crush: A FORTRAN program for the analysis of the rigid unit mode spectrum of a framework structure. *Am. Mineral.* 79 (11-12), 1207–1209.
- Hammonds, K.D., Dove, M.T., Giddy, A.P., Heine, V., Winkler, B., 1996. Rigid-unit phonon modes and structural phase transitions in framework silicates. *Am. Mineral.* 81 (9-10), 1057–1079.
- Heine, V., Welche, P.R.L., Dove, M.T., 1999. Geometrical origin and theory of negative thermal expansion in framework structures. *J. Am. Ceram. Soc.* 82 (7), 1793–1802.
- Kramer, G.J., Farragher, N.P., van Beest, B.W.H., van Santen, R.A., 1991. Interatomic force fields for silicas, aluminophosphates, and zeolites: derivation based on ab initio calculations. *Phys. Rev., B* 43 (6), 5068–5080.
- Sartbaeva, A., Wells, S.A., Redfern, S.A.T., 2004. Li<sup>+</sup> ion motion in quartz and  $\beta$ -eucryptite studied by dielectric spectroscopy and atomistic simulations. *J. Phys., Condens. Matter* 16 (46), 8173–8189.
- Welche, P.R.L., Heine, V., Dove, M.T., 1998. Negative thermal expansion in beta-quartz. *Phys. Chem. Miner.* 26 (1), 63–77.
- Wells, S.A., 2004. GASP: Geometric Analysis of Structural Polyhedra. [http://exweb.la.asu.edu/gasp/gasp\\_index.html](http://exweb.la.asu.edu/gasp/gasp_index.html).
- Wells, S.A., Dove, M.T., Tucker, M.G., Trachenko, K., 2002. Real-space rigid-unit-mode analysis of dynamic disorder in quartz, cristobalite and amorphous silica. *J. Phys., Condens. Matter* 14 (18), 4645–4657.
- Wells, S.A., Dove, M.T., Tucker, M.G., 2004. Reverse Monte Carlo with geometric analysis—RMC+GA. *J. Appl. Cryst.* 37 (4), 536–544.